Electronic Supplementary Material (ESI) for Soft Matter.

Supplementary Information for Active self-assembly of colloidal machines with passive rotational parts via coordination of phoresis and osmosis

Nan Yu,[1,2] Zameer Hussain Shah,[1,2] Majid Basharat,[1,2] Shuo Wang,[1,2] Xuemao Zhou,[1,2] Guanhua Lin,[1] Scott A. Edwards,[1] Mingcheng Yang,[3,4,5,*] and Yongxiang Gao[1,†]

[1]*Institute for Advanced Study, Shenzhen University, 518060, Shenzhen, China*

[2]*Key Laboratory of Optoelectronic Device and Systems of Ministry of Education and Guangdong Provice, College of Optoelectronic Engineering, Shenzhen University, 518060, Shenzhen, China*

[3]*Beijing National Laboratory for Condensed Matter Physics and Laboratory of Soft Matter Physics, Institute of Physics, Chinese Academy of Sciences, Beijing 100190, China*

[4]*School of Physical Sciences, University of Chinese Academy of Sciences, Beijing 100049, China*

[5]*Songshan Lake Materials Laboratory, Dongguan, Guangdong 523808, China*

1. Scanning electron microscopy images of colloids

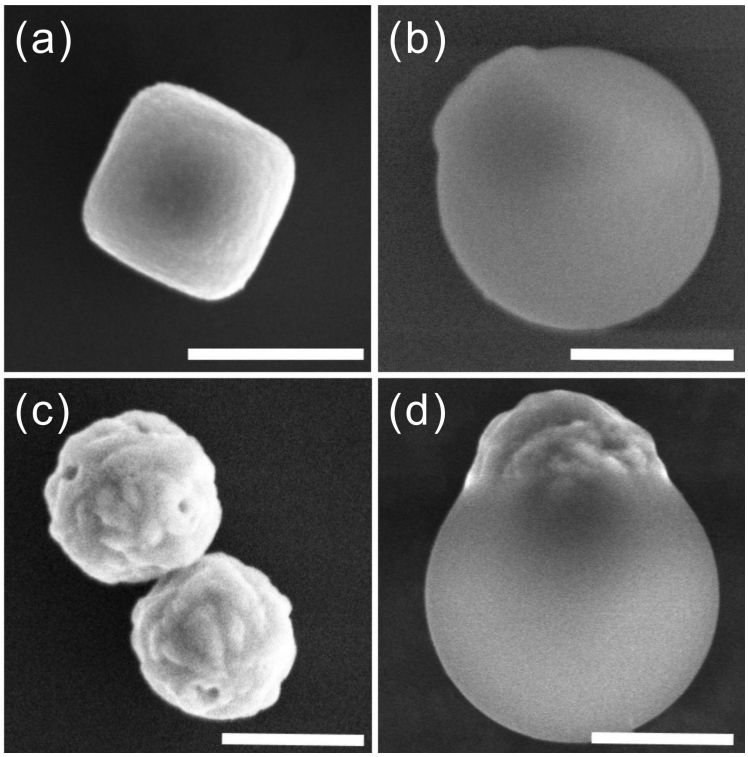

FIG. S1. SEM images of (a) a hematite cube, (b) a hematite-TPM Janus colloid, (c) Ag colloids, and (d) an Ag-TPM Janus colloid. Scalebars are 1 μm.

2. ζ-potential measurement of colloidal particles

The ζ-potential of colloids were measured by preparing a dilute suspension of particles with a volume fraction $\sim 10^{-5}$ in Deionized water right before measurements with a Zetasizer (NanoBrook 90PlusPALS), which has a measurement range for particles with a diameter between 1 nm and 10 μm and a ζ-potential between -500 mV and 500 mV. The reported results were all averaged over three measurements for each sample, which were completed in 3 minutes.

* mcyang@iphy.ac.cn
† yongxiang.gao@szu.edu.cn

3. Sizes and zeta-potentials of Ag-TPM and hematite-TPM Janus colloid

Table 1. D_{Ag}, D_{hem} and D_{TPM} represent the diameter of Ag, hematite and TPM part, respectively. R represents the center-to-center separation.

Ag-TPM	ζ-potential (mV)	-43 ± 3	Hematite-TPM	ζ-potential (mV)	-35 ± 2
	D_{Ag} (μm)	1.20 ± 0.14		D_{hem} (μm)	1.00 ± 0.04
	D_{TPM} (μm)	1.90 ± 0.12		D_{TPM} (μm)	1.78 ± 0.08
	R (μm)	0.92 ± 0.13		R (μm)	0.39 ± 0.04

4. Motion of a passive colloid when it is not at one of the two preferred binding sites

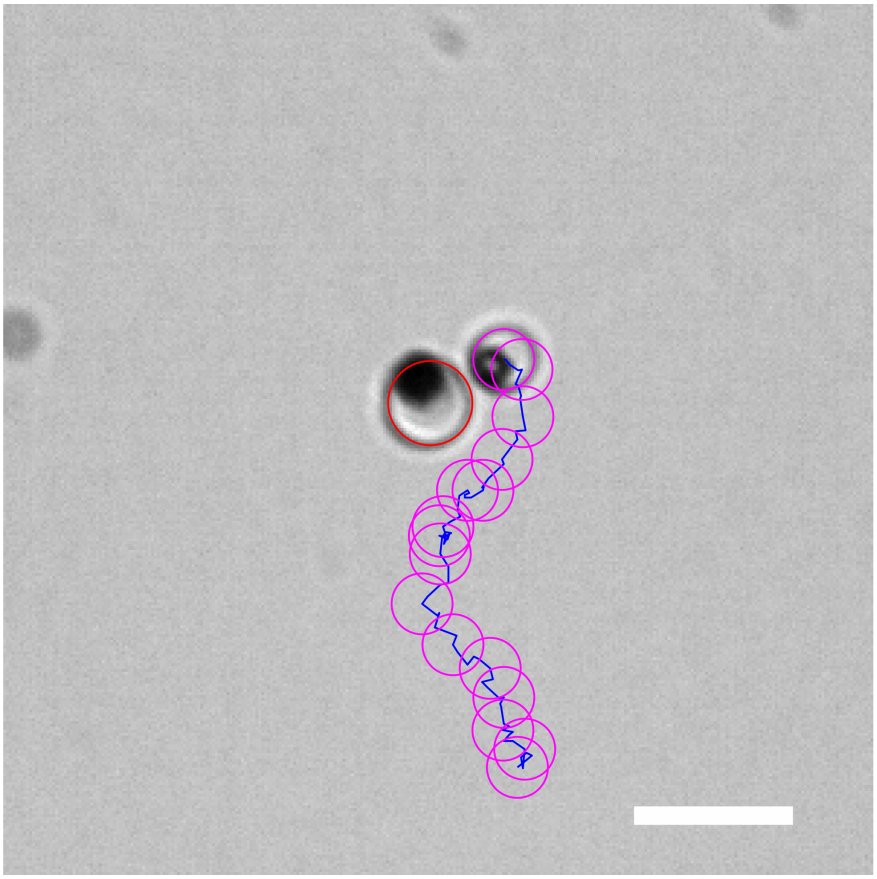

FIG. S2. Motion of a passive colloid when it is not at one of the two preferred binding sites. Red circle indicates the position and the size of the active colloid; purple circles indicate the location of the passive colloids every 1 second; the blue solid line shows the trajectories of the passive colloid over a period of 15 seconds. The scalebar is 5 μm.

5. Finite element analysis on the chemical, electric and flow fields

To simulate the chemical reactions, the fluxes of ions J_0 were set to be $-D_{\pm}\nabla c \cdot n$ and 0 at the active and the inert surfaces, respectively. Here, c and $D_{\pm}$ are the concentration and the diffusion coefficient of the produced electrolyte, with $D_{\pm} = 2D_{+}D_{-}/(D_{+}+D_{-})$. D_{+} and D_{-} are set to be the diffusion coefficients of Ag^{+} and OH^{-}, which are $1.65 \times 10^{-9} m^2 s^{-1}$ and $5.273 \times 10^{-9} m^2 s^{-1}$, respectively [1]. Their high contrast in diffusivity can properly account for between anions and cations and the negligible contribution from chemical gradients of neutral species such as O_2 and H_2O_2 in self-diffusiophoresis of active colloids estimated previously [2–6], only ionic species were considered here. The concentration field is described by the steady state diffusion equation, $\nabla \cdot (D_{\pm}\nabla c) = 0$, with $c = 0$ far from the particle. The flow field is governed by the stokes equation, $-\nabla P + \eta \Delta u = 0$, with P the pressure, η the fluid viscosity, and $\nabla \cdot u = 0$, assuming the fluid to be incompressible. The concentration gradient induces a slip velocity at the particle/solution interface according to the equation [7],

$$v^s = \left[-\frac{\varepsilon\zeta}{4\pi\eta}\frac{k_B T}{e}\frac{D_{+}-D_{-}}{D_{+}+D_{-}} + \frac{\varepsilon}{2\pi\eta}\left(\frac{k_B T}{e}\right)^2 \ln\left(1-\tanh^2\left(\frac{e\zeta}{4k_B T}\right)\right)\right] \nabla(\ln c)\cdot(I-nn), \tag{1}$$

6. Mesoscale computer simulations

In mesocale fluid simulations, we use coarse-grained method to model the solvent as a large number N of point-like particles of mass m with continuous positions $r_i(t)$ and velocities $v_i(t)$. The algorithm consists of alternating streaming and collision steps. In the streaming step, all the solvent particles move ballistically for a time h. In the collision step, particles are sorted into a square lattice with lattice size a, and interchange momentum relative to the center-of-mass velocity of each collision cell. In our simulations the stochastic rotation collision rule with variable collision angle α introduced by Ryder and Yeomans [8, 9] is employed. This collision rule locally conserves mass, linear momentum, energy and angular momentum. It can therefore be proved that the algorithm properly captures hydrodynamic interactions, mass diffusion, thermal fluctuations and thermal conduction. In the simulations we take $a = 1$, $m = 1$, the system mean temperature $k_B T = 0.7$

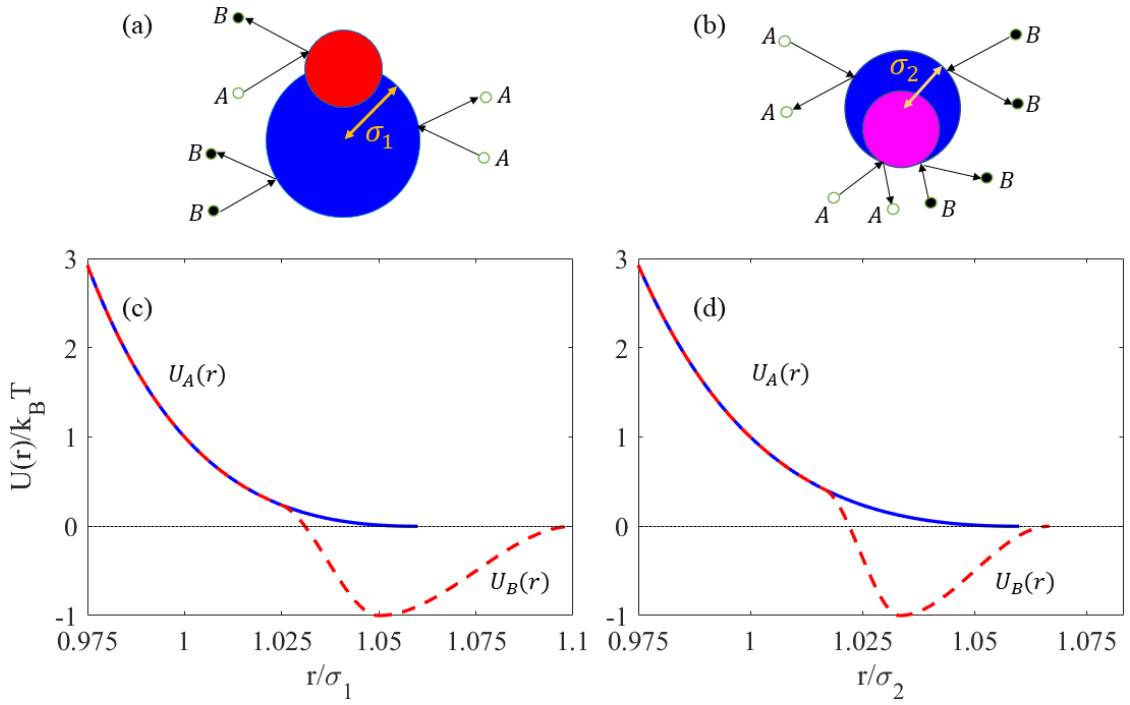

FIG. S3. Schematic representation of the catalytic (red bead) and non-catalytic (blue bead) parts of the active Ag-TPM Janus colloid (a) and the passive hematite-TPM colloid (b). The chemical reaction A $\rightarrow$ B happens on the surface of the catalytic part of the active Janus particle. (c) Potential interactions of the non-catalytic part of the active Janus colloid with solvent species A ($U_A(r)$ blue solid line) and species B ($U_B(r)$ red dashed line). (d) Potential interactions of the passive colloidal particle with solvent species A (blue solid line) and species B (red dashed line). Here, $U_A(r)$ is purely repulsive, while $U_B(r)$ has an attractive tail.

with k_B being the Boltzmann constant, the time step $h = 0.1$, and the mean number of solvent particles per cell $\rho = 50$.

To mimick the catalytic reaction on the surface of the active particle, we consider the solvent contains two species A (reactant) and B (product). When species A approaches to the catalytic surface of the active colloid, it will turn into species B with a reaction probability $p = 1$; while inverse reaction far away from the colloids is implemented in order to input the fuel, with a reaction probability $p = 0.0025$. Solvent species A and B interact with the colloids through different potentials, as displayed in Fig. S3. The interactions of species A with the non-catalytic part of the active colloid and the passive colloid are both described by a truncated and shifted Lennard-Jones potential, $U_A(r) = 4\varepsilon[(\sigma/r)^{24} - (\sigma/r)^{12}] + \varepsilon$, for $r \leq r_c$, but with different particle radius σ. Here, r is the distance from the colloid center to the solvent molecules, $\varepsilon = 1$ is the potential intensity, and r_c is the corresponding interaction range. While, solvent species B interacts with the passive colloid

and the non-catalytic part of the active particle via $U_B(r)$, which is constructed from the repulsive Lennard-Jones potential $U_A(r)$ using a cubic spline interpolation, producing an attractive tail. The interactions between the catalytic part of the active Janus particle and the two solvent species (A and B) are the same repulsive Lennard-Jones potential. The colloidal particles and their neighbouring solvent evolve according to molecular dynamics scheme, in which the particle equations of motion are integrated by the velocity-Verlet algorithm with a time step $\Delta t = h/50$.

7. Guide to Supplementary Videos

Supporting Video S1: Video shows the spinning dynamics of the assembly of a passive colloid with a fixed active colloid.

Supporting Video S2: Video shows the co-rotating dynamics of the assembly of a passive colloid with a semi-fixed active colloid.

Supporting Video S3: Video shows orbiting of a free active colloid around a passive colloid and the oppositely spinning of two passive colloids carried by an active colloid.

Supporting Video S4: Video shows the motion of a passive colloid when it is not at one of the two preferred binding sites.

Movies S1-S4 are played at 2× of real time. Scalebars are 2 μm.

Supporting Video S5: Video shows the simulation results of rotary colloidal machines composed of (a) a passive colloid with a fixed active colloid, (b) a passive colloid with a semi-fixed active colloid, (c) a passive colloid with a free active colloid, and (d) two passive colloids with a free active colloid. Passive colloids are as Janus particles only for visualization purpose.

---

[1] Z. Shah, S. Wang, L. Xian, X. Zhou, Y. Chen, G. Lin, and Y. Gao, Chem. Commun. **56**, 15301 (2020).

[2] D. Velegol, A. Garg, R. Guha, A. Kar, and M. Kumar, Soft Matter **12**, 4686 (2016).

[3] A. Brown and W. Poon, Soft Matter **10**, 4016 (2014).

[4] X. Zhou, S. Wang, L. Xian, Z. H. Shah, Y. Li, G. Lin, and Y. Gao, Phys. Rev. Lett. **127**, 168001 (2021).

[5] A. I. Campbell, S. J. Ebbens, P. Illien, and R. Golestanian, Nat. Commun. **10**, 3952 (2019).

[6] X. Lyu, X. Liu, C. Zhou, S. Duan, P. Xu, J. Dai, X. Chen, Y. Peng, D. Cui, J. Tang, et al., J. Am. Chem. Soc. **143**, 12154 (2021).

[7] D. Prieve, J. Anderson, J. Ebel, and M. Lowell, J. Fluid. Mech. **148**, 247 (1984).

[8] J. F. Ryder, *Mesoscopic Simulations of Complex Fluids* (Ph.D. thesis, University of Oxford, 2005).

[9] G. Gompper, T. Ihle, D. Kroll, and R. Winkler, Adv. Polym. Sci. **221**, 1 (2009).